Gulf and Caribbean Research

Volume 32 | Issue 1

2021

Spatial Variability of Sediment Amorphous Silica and its Reactivity in a Northern Gulf of Mexico Estuary and Coastal Zone

Elliot J. Kemp
Lyon College, skemp0408@gmail.com

Ryan R. Roseburrough
University of South Alabama, rroseburrough@disl.org

Emily A. Elliott
University of Alabama, emily.elliott@ua.edu

Jeffrey W. Krause
Dauphin Island Sea Lab, jkrause@disl.org

Recommended Citation

Kemp, E. J., R. R. Roseburrough, E. A. Elliott and J. W. Krause. 2021. Spatial Variability of Sediment Amorphous Silica and its Reactivity in a Northern Gulf of Mexico Estuary and Coastal Zone. Gulf and Caribbean Research 32 (1): SC6-SC11.
Retrieved from https://aquila.usm.edu/gcr/vol32/iss1/14
DOI: https://doi.org/10.18785/gcr.3201.14

GULF AND CARIBBEAN

RESEARCH

Volume 32
2021
ISSN: 2572-1410

Published by

THE UNIVERSITY OF
SOUTHERN MISSISSIPPI

GULF COAST RESEARCH LABORATORY
Ocean Springs, Mississippi

Gulf and Caribbean Research Vol 32, SC6-SC11, 2021
DOI: 10.18785/gcr.3201.14
Manuscript received September 16, 2021; accepted November 20, 2021

SHORT COMMUNICATION

SPATIAL VARIABILITY OF SEDIMENT AMORPHOUS SILICA AND ITS REACTIVITY IN A NORTHERN GULF OF MEXICO ESTUARY AND COASTAL ZONE§

Elliot J. Kemp[1,2], Ryan R. Roseburrough[2,3], Emily A. Elliott[4,5], Jeffrey W. Krause[2,3]*
*[1]Lyon College, 2300 Highland Road, Batesville, AR, 72501 USA; [2]Dauphin Island Sea Lab, 101 Bienville Boulevard, Dauphin Island, AL, 36528 USA; [3]School of Marine and Environmental Sciences, University of South Alabama, 600 Clinic Drive, Suite 300, Mobile, AL, 36608, USA; [4]Department of Geography, University of Alabama, Tuscaloosa, AL, USA; [5]Department of Geological Sciences, University of Alabama, 201 7th Avenue, Tuscaloosa, AL, 35487, USA; *Corresponding author, email: jkrause@disl.edu*

KEY WORDS: silica cycle, sediment, diagenesis, amorphous silica, biogenic silica

INTRODUCTION

Diatom—associated material is important for both biotic and abiotic processes controlling the marine silica cycle. Diatoms are a group of phytoplankton which have an obligate requirement for dissolved silica to make their amorphous silica (ASi) shells (also known as biogenic silica). They are responsible for 20—40% of marine primary production and thereby link the marine silica and carbon cycles (Ragueneau et al. 2000). Once diatoms die and sink into the sediment, their ASi shells dissolve or can be transformed by diagenesis. The former can introduce solubilized silica back into the water column to fuel further diatom productivity, whereas the latter can sequester ASi and other elements (e.g., Fe, Al, Mg, K) through the process of reverse weathering (Rahman 2019). Since a byproduct of reverse weathering is CO_2, both diatom activity and abiotic chemical reactions involving diatom ASi play a role in global climate through consumption and production of this greenhouse gas. While the understanding of marine silica cycling has increased in the last decades, there are still many unknowns about processes at the land—sea interface, especially in estuarine systems.

Estuaries not only provide critical habitat and spawning grounds for many economically important species, these zones are biogeochemically active. Prior work has demonstrated that salt marshes can retain ASi, i.e. non—crystalline silica from diatoms, phytoliths, and clays (Carey and Fulweiler 2014), yet the fate of this silica has not been rigorously examined. Physicochemical properties (e.g., temperature) govern ASi dissolution along with the reactivity and exposed area of the surfaces to seawater (e.g., Van Cappellen and Qiu 1997). However, a master variable is the degree of undersaturation in the water for dissolved silica; this drives the dissolution process and is dependent on silica solubility (i.e., its capacity to dissolve). If the sediment ASi solubility is high, then ASi dissolution into porewater and benthic flux back into the water column could fuel additional diatom production; if solubility is low, ASi may become buried, potentially modified by reverse weathering, and sequestered. Incorporation of metals (e.g., Al) into ASi reduces its solubility, and thus estuarine sediments which have high detrital mineral content (Al—rich materials) may have lower ASi solubilities and dissolution rates relative to coastal systems with less detrital material (e.g., Wu and Liu 2020).

We report a study of reactive silica pools in the northern Gulf of Mexico (nGoM), specifically in the Mobile Bay estuary and offshore coastal Alabama sediments. We predict a decrease in total reactive ASi and its solubility from Mobile Bay towards the nGoM due to high detrital mineral content in the estuarine sediments, which would suggest ASi is not recycled efficiently in the estuary. Many studies favor steady—state flow—through reactors for estimating ASi solubility (Wu and Liu 2020); however, prior work has shown solubility rates from batch reactors are ~10% lower relative to those determined from flow—through reactors (Van Cappellen and Qiu 1997). Given the order of magnitude of the ASi solubility range observed in marine environments (e.g., Rickert et al. 2002, Wu and Liu 2020), a 10% agreement among methods is reasonable, thus suggesting a simpler batch approach can provide meaningful data to test our hypothesis using regional sediments.

MATERIALS AND METHODS

Sediment sampling and processing

Sediment cores were taken at 3 stations in Mobile Bay and the nGoM (Figure 1) using an Ocean Instruments 4—spot multi—corer aboard the *R/V Alabama Discovery*. Core penetration was sufficient to extrude material from a depth of 11 cm among stations. Surface water was gently siphoned off and the first samples were taken at 1 cm depth to avoid flocculent surface layers with high porosity (ϕ >0.90). Each core was sectioned at 2 cm intervals, and then sediment was subsampled into 50 mL polypropylene centrifuge tubes and stored on ice. In the laboratory, about 10 g of wet sediment was subsampled into new 50 mL centrifuge tube, freeze—dried, and homog-

§*The first author conducted this research as part of the Dauphin Island Sea Lab's Research Experience for Undergraduates in the coastal and nearshore marine science program.*

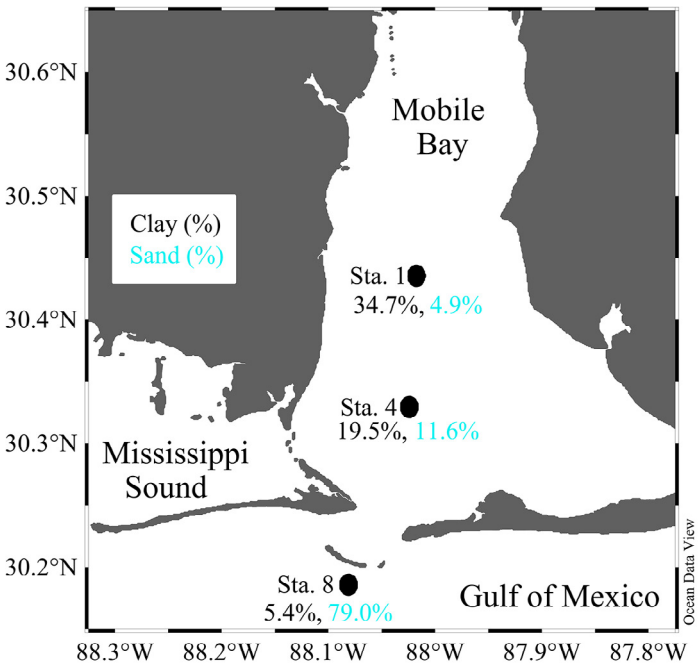

FIGURE 1. *Station locations (black dots) sampled on 4 June 2021 in the Mobile Bay estuary and coastal Alabama northern Gulf of Mexico along with the average clay (diameter <3.9 µm, black font) and sand (diameter >63–2000 µm, cyan color font) grain percentage in the upper 11 cm at each station.*

enized using a mortar and pestle, consistent with prior studies (Wu and Liu 2020); these samples were analyzed for ASi and grain size.

Additional sediment subsamples were analyzed for bulk characteristics. Wet sediment from the original 50 mL tube was subsampled into a pre–weighed polypropylene microcentrifuge tube and filled to a constant volume, then weighed, dried at 60°C for 48 h, and weighed again. Water–weight was the difference before and after drying, and porosity was calculated assuming bulk sediment and water densities of 2.60 and 1.023 g/mL, respectively. Organic matter content was estimated using a loss on ignition method. Briefly, approximately 1 g of the dried sediment was subsampled into an aluminum tin, the tare mass recorded, and the samples were combusted at 550°C for 6 h. After combustion, final masses were taken, and percent organic matter was calculated; we assumed negligible contribution from carbonates in these locations (Davis 2017).

Amorphous silica and its solubility

Two reactive sediment silica pools were quantified using established approaches (Michalopoulos and Aller 2004, Krause et al. 2017, Pickering et al. 2020). To determine the amount of reactive ASi associated with early diagenetic products (e.g., metal oxide coatings and/or clays, hereafter referred to as Si–HCl), a mild acid leach was performed. For each station and depth, replicate freeze–dried 0.05 g sediment subsamples were placed into new 50 mL polypropylene centrifuge tubes. Prior studies (Michalopoulos and Aller 2004, Krause et al. 2017, Pickering et al. 2020) used frozen samples; however, we chose to use freeze–dried material for consistency with solubility measurements reported in other studies (e.g., Wu and Liu 2020). Briefly, a mild acid leach was achieved by adding 36 mL of 0.1 N HCl to each tube and the placing all tubes on a shaker table for 18 h at room temperature. After leaching, tubes were centrifuged, and 35 mL of the supernatant was removed for analysis of solubilized silica using a colorimetric molybdate method. The remaining 1 mL of supernatant was diluted with 18.2 MΩ deionized water, centrifuged, and aspirated. Following this, 25 mL of 0.1 M $NaCO_3$ was added to each tube, tubes were placed in a water bath (85°C), and digestions were subsampled (1.0 mL) over 5 h. Subsamples were diluted and analyzed for solubilized silica, as described above. The y–intercept of solubilized silica vs. digestion time (e.g., >1 h) denotes the initial ASi content associated with organism silica (collectively referred to as Si–Alk) in the absence of lithogenic interference.

To determine ASi solubility, 1 g of freeze–dried sediment was transferred into triplicate 50 mL polypropylene centrifuge tubes. Sediment was resuspended in 50 mL of Aquil artificial seawater (Morel et al. 1979) and placed on a shaker table. Tubes were subsampled (0.5 mL) at multiple time points over 46 d to quantify the increase in dissolved silica over time.

Statistical analyses were done using SigmaPlot software. Dissolved silica concentrations over time were fit to a rectangular hyperbola using a non–linear regression curve fitting algorithm. The asymptote of the hyperbola (in concentration units) was assumed to be the apparent solubility concentration; all non–linear regressions were highly significant (adjusted r^2 range 0.87 – 0.99, $p < 0.001$ for the regression fit). Solubility data were analyzed using a linear regression with solubility as the dependent variable and the Si–HCl:Si–Alk ratio as the independent variable; data passed a Shapiro–Wilk normality test (alpha = 0.05).

Results and Discussion

Sediment characteristics

Sediment characteristics varied greatly at each station. In the nGoM station (station 8), depths 1–7 cm had a higher sand content than the Bay stations (stations 1 and 4; Figure 1) as well as the deeper sediment layers at this station (Supplemental Table S1). These grain size differences corresponded well with spatial and vertical variation in water content and porosity (Figure 2); specifically, both measurements were lower at station 8 than at stations 1 or 4. Similarly, the organic matter mass percentage in the Bay stations 1 and 4 (6–7%) was 4–fold higher than in the nGoM station 8 (~1.5%, Supplemental Table S1), consistent with prior regional studies (Davis 2017). The high percentages of sand at nGoM station 8 could be due to its proximal distance from the shoreline or from redistributed offshore and adjacent shoreface sediments deposited in this location during the 2020 hurricane season. Hurricane Sally's (September 2020) eyewall was centered over all stations. This storm rapidly intensified and moved slowly; consequently, an exceptional amount of precipitation accumulated (up to 76 cm in the vicinity of station 8) in <2 days (Berg and Reinhard 2021). A second hurricane, Zeta, came through the region in October 2020 and made landfall to the west, but a 1–2 m

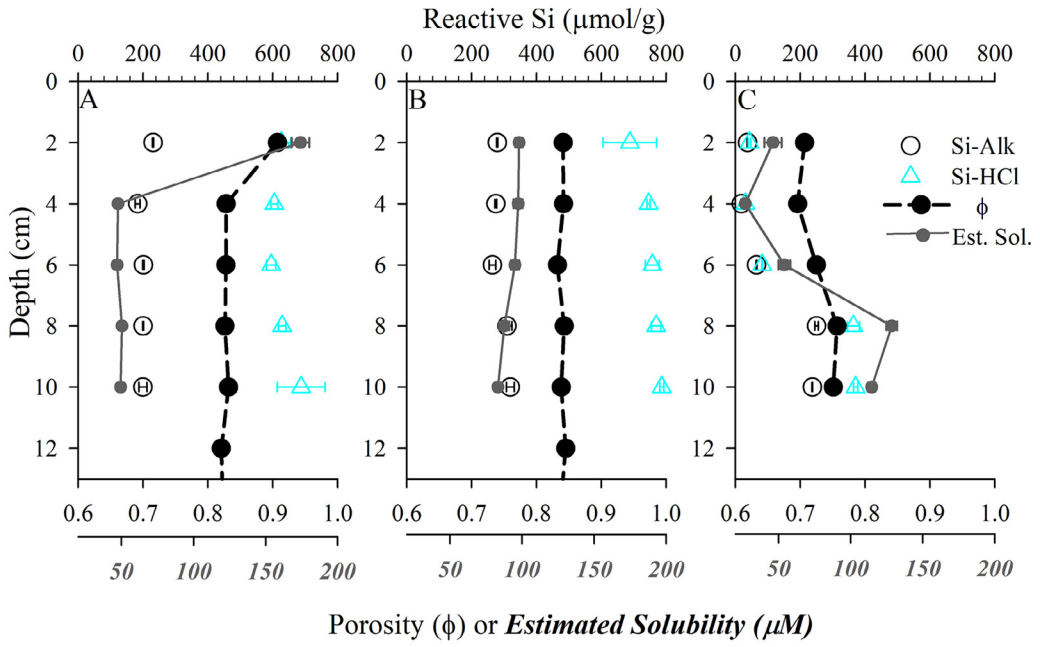

FIGURE 2. *Station and vertical variability in sediment reactive amorphous silica (top scale) including Si—HCl (cyan triangles) and Si—Alk pools (open circles), sediment porosity (ϕ, black filled circles, lower scale normal font), and estimated amorphous silica solubility (Est. Sol., gray filled smaller circles, lower scale bold/italicized font). Data expressed as mean ± se. A. Mobile Bay station 1. B. Mobile Bay station 4. C. Northern Gulf of Mexico station 8.*

storm surge occurred that impacted our stations (Blake et al. 2021). Thus, the top layer of sand at the nGoM station likely was associated with storm—induced flooding, suggesting rapid post—storm deposition between September and November 2020.

Sediment silica pools

Spatial and vertical variability in reactive ASi pools correlated to sediment characteristics. In the Bay stations, Si—Alk ranged from 183–319 µmol/g (mean ± se, 246 ± 16; Figure 2A, B). At the nGoM station 8 there was a decline of Si—Alk in the upper 7 cm, with a mean of 40 ± 14 µmol/g, but between >7–11 cm, Si—Alk measurements were comparable to the bay stations, 244 ± 6 µmol/g (Figure 2C). Similar spatial differences were observed in Si—HCl, with Bay stations 1 and 4 ranging from 595– 86 µmol/g (mean 689 ± 23) with lower contents in the upper 7 cm at nGoM station 8, averaging 53 ± 16 µmol/g (Figure 2). Si—HCl contents in the deeper depths of station 8 were ~50% of that observed in the bay stations, averaging 367 ± 3 µmol/g.

Bay stations 1 and 4 had much higher ASi content than reported in other estuaries. Measurements of Si—Alk and Si—HCL in Mississippi Sound, fed by water from Mobile Bay (Figure 1), are up to 82 µmol/g and 45 µmol/g, respectively (Krause et al. 2017). Bay stations 1 and 4 also show higher levels of both Si—Alk and Si—HCl than found in the Yangtze River estuary (China), with a range of <50–200 µmol/g for Si—Alk and 25–85 µmol/g for Si—HCl (Wang et al. 2015) and the Pearl River estuary (China), with a range of 150–240 µmol/g for Si—Alk and 80–90 µmol/g for Si—HCl (Qin et al. 2012). Our quantified Si—Alk values are also among the higher values reported in more temperate latitude estuaries, e.g. Chesapeake Bay (United States) and Wadden Sea (Germany), which range from 90–400 µmol/g (Barão et al. 2015). Furthermore, these silica pools match or exceed major river plume systems like the Amazon River (100–235 µmol/g for Si—Alk and 90–150 µmol/g for Si—HCl, Michalopoulos and Aller 2004) and Mississippi River (73–444 µmol/g for Si—Alk and 111–390 µmol/g for Si—HCl, Presti and Michalopoulos 2008).

Sand—dominated sediments altered the composition and magnitude of reactive ASi among stations. The sediment—reactive ASi among sand—dominated depths (e.g., upper 7 cm of nGoM station 8) was an order of magnitude lower than corresponding depths at Bay stations with lower sand content and higher porosity (Figure 2). However, reactive ASi in sandy sediments from this study were an order of magnitude higher than Si—Alk and Si—HCl reported by Ehlert et al. (2016) in North Sea coastal sandy sediments (range 1–4 µmol/g for both Si—Alk and Si—HCl). While our trends are consistent with broader results from other systems of lower ASi content in sandy sediments vs. clay and silt—dominated sediments (e.g., Ehlert et al. 2016), our limited data suggest that the nGoM sandy sediments may have higher ASi content compared to similar sediment types in other regions.

The systematically higher ASi compared to prior studies (e.g., Krause et al. 2017) suggests that either nGoM sediments sequester more silica or the additional handling (freeze drying, grinding) of our method may have increased the yield. Recent work has shown that analysis of dried sediments or dried and ground sediments can lead to 2.5—fold reductions or 50% increases, respectively, in quantified ASi relative to analysis using frozen sediment samples (Ward et al. 2021). Given the nearly order of magnitude increases in Si—Alk and Si—HCl reported here relative to other studies and regions, we suggest this methodological difference may not be solely responsible for these trends; thus, we presume that the Mobile Bay region may more efficiently sequester ASi compared to other regions examined to date.

Amorphous silica solubility

The ASi solubility may explain the trend of higher ASi in Mobile Bay compared to other regions. The estimated ASi

solubility was variable among stations and depths (Figure 2). At Bay station 1, the estimated solubility in the top 2 cm was 174 ± 6 µM, whereas estimated solubilities in the rest of the core were lower and similar, i.e. 47–50 µM (Figure 2A). The surface depth also had anomalously high porosity relative to all other stations (Figure 2), which may have been associated with fresh ASi (e.g. water column diatoms) and more reactive than presumably older ASi found deeper in the sediments (Rickert et al. 2002). At Bay station 4, all depths had a higher estimated ASi solubility than the deeper depths at Bay station 1, 83–98 µM (Figure 2B). The nGoM station 8 was the most variable, with estimated solubilities ranging from 27–129 µM among depths (Figure 2C).

The estimated ASi solubility values among stations were lower than values reported from other systems. In the East China Sea, offshore of large river systems, apparent solubilities range from ~200–325 µM (Wu and Liu 2020). However, in the Yellow Sea, reported solubilities range from ~90–300 µM (Wu et al. 2017); the lower end of this range is consistent with our findings. Our ASi solubilities are also lower than those reported for deep ocean sediments, e.g. 500–900 µM from the Southern Ocean (Van Cappellen and Qiu 1997), or for water column diatoms, e.g. >1500 µM (Rickert et al. 2002).

The spatial variability in estimated ASi solubility within Mobile Bay and the nGoM could be due to incorporation of dissolved metals from detrital clay remineralization within the bay sediments. Incorporation of dissolved detrital sourced elements into the diatom ASi matrix reduces the apparent solubility (Dixit et al. 2001). The increased fraction of lithogenic material in sediments has been shown to be negatively correlated to sediment silica solubility (Van Cappellen and Qiu 1997, Wu and Liu 2020), and this may be approximated by the ratio of detrital silica (e.g., Si—HCl) to organism ASi (e.g., Si—Alk). Plotting our estimated solubility data vs. the Si—HCl to Si—Alk ratio (Figure 3) shows a negative linear trend (adjusted r^2 = 0.77) among sediments with high clay/detrital content (e.g., Bay stations 1, 4, and deeper depths in nGoM station 8). This suggests that the solubility differences among our stations and depths could be due to dissolution and incorporation of detrital metals into the organism ASi or coatings by metal—oxide precipitates which reduce the effective surface area of the diatom silica that can react with silica—undersaturated seawater.

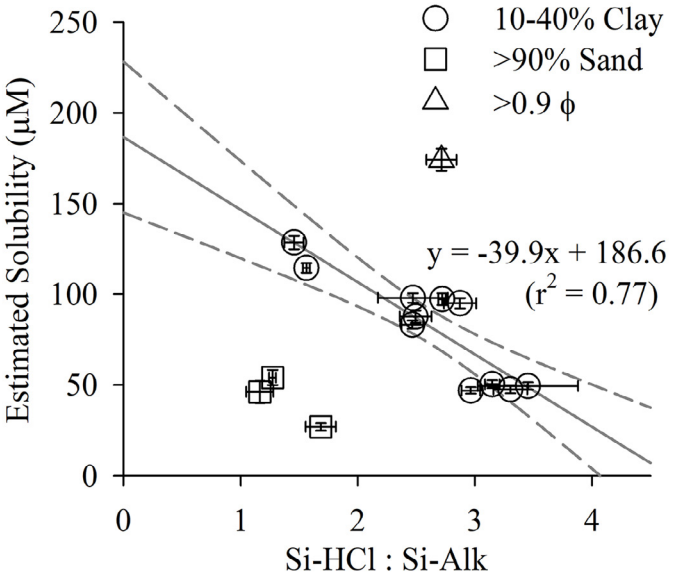

FIGURE 3. *Sediment amorphous silica solubility as a function of sediment lithogenic to amorphous silica content, approximated by the ratio of Si—HCl (e.g., metal oxide silica, sourced from detrital material) to Si—Alk (e.g. organism ASi). Symbols represent mean ± se. Linear regression (solid gray line, dashed gray lines are 95% confidence intervals, adjusted r^2 = 0.77) was made to only the circular symbols, as other depths were dominated by sand (squares) or had anomalously high porosity (triangle) relative to other depths and stations. Regression coefficients (slope, intercept) were both significantly different from zero ($p < 0.002$) and data passed a Shapiro—Wilk normality test ($p < 0.05$).*

Gulf of Mexico river—dominated estuaries as major ASi accumulation zones

Comparison to other estuaries, both within the nGoM and other systems, suggest that river—dominated estuaries such as Mobile Bay may act as major accumulation zones for ASi, consistent with the hypothesis in Michalopoulos et al. (2000). Despite similar Si—Alk in Mobile Bay stations and the deeper depths of the nGoM station, estimated ASi solubilities measured in the estuary were 40–76% of that in deeper depths of the nGoM station. The reduced solubility in Mobile Bay suggests that remineralization is minimized in these sediments; therefore, the fate of most ASi exported to these sediments is burial instead of dissolution and flux back into the water column. Further analysis to determine the type of ASi, its geographical origin, and whether metal—heavy precipitates form onto, or metals are incorporated within, the ASi will help increase understanding of the mechanism(s) by which river—dominated estuaries and adjacent coastal zones can accumulate sediment ASi. Furthermore, since climate projections strongly suggest increasing precipitation in the future (e.g., Warwick et al. 2018), thereby increasing riverine discharge, understanding these mechanisms will help determine whether increasing sediment loads (e.g. detrital material source) will increase the magnitude of this ASi accumulation in estuarine systems and how this will affect the linkage to other biogeochemical cycles.

Acknowledgements

The Dauphin Island Sea Lab's Research Experience for Undergraduates in coastal and nearshore marine science program was funded by the National Science Foundation award OCE—1838618. Additional support for this research was provided from OCE—1924585. Grainsize analysis was conducted through collaboration with the University of Alabama Collaborative Research on Paleoenvironments and Societies. We thank W. Bird, M. Boehm, W. Clemo, D. Cole, K. Dorgan, J. Goff, G. Lockridge, A. Robertson and A. Smith for laboratory and technical assistance, and R. Carmichael and J. Gwinn for program assistance.

Literature Cited

Barão, L., F. Vandevenne, W. Clymans, P. Frings, O. Ragueneau, P. Meire, D.J. Conley, and E. Struyf. 2015. Alkaline—extractable silicon from land to ocean: A challenge for biogenic silicon determination. Limnology and Oceanography: Methods 13:329—344. https://doi.org/10.1002/lom3.10028

Berg, R. and B.J. Reinhard. 2021. Hurricane Sally (AL192020). Tropical Cyclone Reports, National Hurricane Center, Maimi, FL, USA. 69 pgs. https://www.nhc.noaa.gov/data/tcr/AL192020_Sally.pdf

Blake, E., R. Berg, and A. Hagen. 2021. Hurricane Zeta (AL282020). Tropical Cyclone Reports, National Hurricane Center, Maimi, FL, USA. 56 pgs. https://www.nhc.noaa.gov/data/tcr/AL282020_Zeta.pdf

Carey, J. and R. Fulweiler. 2014. Salt marsh tidal exchange increases residence time of silica in estuaries. Limnology and Oceanography 59:1203—1212. https://doi.org/10.4319/lo.2014.59.4.1203

Davis, R.A. 2017. Sediments of the Gulf of Mexico. In: C.H. Ward, ed. Habitats and Biota of the Gulf of Mexico: Before the Deepwater Horizon Oil Spill, Volume 1. Springer, New York, NY, USA, p. 165—215. https://doi.org/10.1007/978—1—4939—3447—8

Dixit, S., P. Van Cappellen, and A.J. van Bennekom. 2001. Processes controlling solubility of biogenic silica and pore water build—up of silicic acid in marine sediments. Marine Chemistry 73:333—352. https://doi.org/10.1016/S0304—4203(00)00118—3

Ehlert, C., A. Reckhardt, J. Greskowiak, B.T.P. Liguori, P. Böning, R. Paffrath. H.J. Brumsack, and K. Pahnkea. 2016. Transformation of silicon in a sandy beach ecosystem: Insights from stable silicon isotopes from fresh and saline groundwaters. Chemical Geology 440:207—218. https://doi.org/10.1016/j.chemgeo.2016.07.015

Krause, J.W., E.S. Darrow, R.A. Pickering, R.H. Carmichael, A.M. Larson, and J. Basaldua. 2017. Reactive silica fractions in coastal lagoon sediments from the northern Gulf of Mexico. Continental Shelf Research 151:8—14. https://doi.org/10.1016/j.csr.2017.09.014

Michalopoulos, P. and R.C. Aller. 2004. Early diagenesis of biogenic silica in the Amazon delta: Alteration, authigenic clay formation, and storage. Geochimica Et Cosmochimica Acta 68:1061—1085. https://doi.org/10.1016/j.gca.2003.07.018

Michalopoulos, P., R.C. Aller, and R.J. Reeder. 2000. Conversion of diatoms to clays during early diagenesis in tropical, continental shelf muds. Geology 28:1095—1098. https://doi.org/10.1130/0091—7613(2000)28<1095:CODTCD>2.0.CO;2

Morel, F.M., J. Rueter, D.M. Anderson, and R. Guillard. 1979. Aquil: A chemically defined phytoplankton culture medium for trace metal studies. Journal of Phycology 15:135—141. https://doi.org/10.1111/j.1529—8817.1979.tb02976.x

Pickering, R.A., L. Cassarino, K.R. Hendry, X.L. Wang, K. Maiti, and J.W. Krause. 2020. Using stable isotopes to disentangle marine sedimentary signals in reactive silicon pools. Geophysical Research Letters 47:e2020GL087877. https://doi.org/10.1029/2020GL087877

Presti, M. and P. Michalopoulos. 2008. Estimating the contribution of the authigenic mineral component to the long—term reactive silica accumulation on the western shelf of the Mississippi River Delta. Continental Shelf Research 28:823—838. https://doi.org/10.1016/j.csr.2007.12.015

Qin, Y.—C., H.—X. Weng, H. Jin, J. Chen, and R.—X. Tian. 2012. Estimation of authigenic alteration of biogenic and reactive silica in Pearl River estuarine sediments using wet—chemical digestion methods. Environmental Earth Sciences 65:1855—1864. https://doi.org/10.1007/s12665—011—1168—8

Ragueneau, O., P. Tréguer, A. Leynaert, R.F Anderson, M.A. Brzezinski, D.J. DeMaster, R.C. Dugdale, J. Dymond, G. Fischer, R. François, C. Heinze, E. Maier—Reimer, V. Martin—Jézéquel, D.M. Nelson, and B. Quéguiner. 2000. A review of the Si cycle in the modem ocean: Recent progress and missing gaps in the application of biogenic opal as a paleoproductivity proxy. Global and Planetary Change 26:317—365. https://doi.org/10.1016/S0921—8181(00)00052—7

Rahman, S. 2019. Reverse weathering reactions in marine sediments. In: J.K. Cochran, H. Bokeniewicz, and P. Yager, eds. Encyclopedia of Ocean Sciences, 3rd Edition. Academic Press, Cambridge, MA, USA, p. 216—227. https://doi.org/10.1016/B978—0—12—409548—9.10835—8

Rickert, D., M. Schlüter, and K. Wallmann. 2002. Dissolution kinetics of biogenic silica from the water column to the sediments. Geochimica et Cosmochimica Acta 66:439—455. https://doi.org/10.1016/S0016—7037(01)00757—8

Van Cappellen, P. and L. Qiu. 1997. Biogenic silica dissolution in sediments of the Southern Ocean. I. Solubility. Deep Sea Research II 44:1109—1128. https://doi.org/10.1016/S0967—0645(96)00113—0

Wang, C., H. Zhu, P. Wang, J. Hou, Y. Ao, and X. Fan. 2015. Early

diagenetic alterations of biogenic and reactive silica in the surface sediment of the Yangtze Estuary. Continental Shelf Research 99:1–11. https://doi.org/10.1016/j.csr.2015.03.003

Ward, J., K. Hendry, S. Arndt, J.C. Faust, F.S. Freitas, S.F. Henley, J.W. Krause, C. März, H.C. Ng, and R.A. Pickering. 2021. Stable silicon isotopes uncover a mineralogical control on the benthic silicon cycle in the Arctic Barents Sea. EarthArXiv Preprint. https://doi.org/10.31223/X5F04Z

Warwick, R.M., J.R. Tweedley, and I.C. Potter. 2018. Microtidal estuaries warrant special management measures that recognise their critical vulnerability to pollution and climate change. Marine Pollution Bulletin 135: 41–46. https://doi.org/10.1016/j.marpolbul.2018.06.062

Wu, B. and S. Liu. 2020. Dissolution kinetics of biogenic silica and the recalculated silicon balance of the East China Sea. Science of The Total Environment 743:140552. https://doi.org/10.1016/j.scitotenv.2020.140552

Wu, B., S.M. Liu, and J.L. Ren. 2017. Dissolution kinetics of biogenic silica and tentative silicon balance in the Yellow Sea. Limnology and Oceanography 62:1512–1525. https://doi.org/10.1002/lno.10514